ELSEVIER

Ceramics International 33 (2007) 811–814

CERAMICS INTERNATIONAL

www.elsevier.com/locate/ceramint

Rising crack-growth-resistance behavior of Al_2O_3 based composites toughened with Fe_3Al intermetallic

Li Jia[a,*], Gong Hong-Yu[b], Shi Rui-Xia[a], Yin Yan-Sheng[c]

[a] *Department of Material Science and Engineering, Jinan University, Jinan 250022, China*
[b] *Key Laboratory For Liquid Structure and Heredity of Ministry of Education, Engineering Ceramics Key Laboratory Of Shandong Province, Shandong University, Jinan 250061, China*
[c] *School of Material Science and Engineering, China Ocean University, Qingdao 266003, China*

Received 31 October 2005; received in revised form 8 December 2005; accepted 24 January 2006
Available online 11 May 2006

Abstract

Al_2O_3 based composites containing 5–20 vol.% of Fe_3Al intermetallic second-phase particles were prepared by hot-pressing sintering. Significantly improved fracture toughness (8.1 MPa $m^{1/2}$) and bend strength (860 MPa) were achieved in Al_2O_3/20 vol.% Fe_3Al composite. The R-curve behavior for Al_2O_3/5–20 vol.% Fe_3Al composites was estimated by the indentation-strength method. The quantitative analysis of toughness increment indicates that the improvement was attributed to the crack bridging and residual thermal stress toughening effect. High-resolution transmission electron microscopy (HREM) shows that no micro-crack was observed at the interface due to the small thermal expansion coefficient mismatch, and no reaction phase existed at the interface between Al_2O_3 matrix and Fe_3Al particle.

Keywords: A. Hot-pressing; B. Composites; Alumina; Iron aluminide intermetallic; Toughening; Crack-growth-resistance

1. Introduction

Structural ceramics is characterized by their excellent wear resistance, hardness and chemical stability. However, their actual applications are largely limited by their inherent brittleness. Some successful attempts have been made to improve the fracture toughness by adding secondary intermetallic phases [1–3]. Among the possible ceramic matrices, alumina is a typical material appealing to be toughened. The Fe_3Al intermetallic has been among the most widely studied intermetallics because of their low cost, low density, ease of fabrication and resistance to oxidation and corrosion. These advantages have made it possible to be a candidate for toughening ceramics matrix. Compared to alumina, Fe_3Al intermetallic has lower Young's modulus, higher thermal conductivity as well as thermal expansion coefficient. In principle, Fe_3Al should be inherently ductile at room temperature because as a BCC crystal it may show more than five independent slip systems. However, due to hydrogen embrittlement and DO_3 ordering structural, Fe_3Al may also exhibit brittle fracture. Alloy elements such as B, Ti, Cr were added to increase the Fe_3Al room temperature ductility [4]. Even that, the ductility of Fe_3Al (39 MPa $m^{1/2}$ in air environment [5]) is higher than for Al_2O_3. Furthermore, Fe_3Al intermetallic has theoretical chemical compatibility with Al_2O_3 matrix [6,7]. These characteristics make Fe_3Al intermetallic to be an appropriate secondary phase for toughening Al_2O_3.

The preparation and mechanical properties of Al_2O_3/Fe_3Al composite were studied in the initial work [8]. In this paper, the R-curve behavior, quantitative analysis of toughness increment and interfacial structure were further investigated.

2. Experimental

Fe_3Al powder with a fine grain size (20–50 nm) was prepared by mechanical alloying. Elemental powder mixtures (Fe–28 at.% Al, 4 wt.% Ti) were direct-mechanically milled in a planetary ball mill (Model QM-1SP2, Nanjing University Instrument Plant, Nanjing, China) at room temperature, and testing was conducted under a high-purity argon atmosphere for 70 h, at a rate of 360 rpm (rotations per minute). The ball:powder weight ratio was 10:1. The as-milled powders

* Corresponding author. Tel.: +86 531 82767616; fax: +86 531 87101966.
E-mail address: jiali_717@hotmail.com (J. Li).

0272-8842/$32.00
doi:10.1016/j.ceramint.2006.01.026

were separated by sieving and subjected to ordered heat treatments at 700 °C, then blended with Al_2O_3 powder (1 μm, Hebei Yashida Ceramics Co., Ltd., Zhangjiakou, China), and ball-milled for 30 min. After an appropriate plastic additive had been incorporated, the powder mixtures were shaped in a cold compression mold, under 180 MPa pressure, and hot-press sintered in a multipurpose high-temperature furnace (Fujidenpa Kogyo Co., Ltd., Osaka, Japan) at 1550 °C for 30 min, under 40 MPa pressure, with a heating rate of 50 °C/min and a vacuum level of 3×10^{-3} Pa, then degassed at 550 °C for 30 min. After cooling, the specimens were cut and polished for subsequent examination.

Microstructural investigations were performed using both scanning electron microscopy (SEM; Model S2500, Hitachi Co., Ltd., Tokyo, Japan) and transmission electron microscopy (TEM; Model JEM2000FX, JEOL, Tokyo, Japan). TEM specimens were mechanically ground to a 150 μm thickness, dimpled to 30 μm, and then thinned to perforation by an argon-ion beam. High-resolution transmission electron microscopy observations were carried out (HREM; Model JEM2010, JEOL, Tokyo, Japan). Vickers indentations were made on the polished specimens, with a maximum load of 296 N, held for 15 s, to observe crack propagation. Fracture toughness and bending strength were measured on the polished surfaces of the samples. Fracture toughness tests were performed by the single-edge notched-beam (SENB) method (on specimens 2 mm × 4 mm × 36 mm in size, at a loading rate of 0.5 mm/min, with a span of 20 mm). A straight through notch with a relative length, $a/W = 0.5$ was introduced at the center of the specimens by a diamond blade. Then, the notch root was sharpened to a radius of <6 μm with a razor blade, which was sprinkled with fine diamond paste. Bending strength was measured by the three-point test (on specimens 3 mm × 4 mm × 36 mm in size). Total of six measurements were made and the average value was obtained.

3. Results and discussion

Fig. 1(a) shows a representative microstructure of Al_2O_3/10 vol.% Fe_3Al after hot-press sintering at 1550 °C. A sufficiently homogeneous microstructure was achieved, with Fe_3Al particle sizes ranging from 0.2 μm down to <2 μm. Further information on the microstructure of the studied material was provided by the TEM micrograph (Fig. 1(b)). The average grain size of Al_2O_3 matrix was about 10 μm. In numerous areas fine Fe_3Al particles with average size of 0.4 μm could be noticed in the Al_2O_3 matrix, while larger Fe_3Al particles with size >1 μm mainly located at the grain boundaries.

Table 1
Mechanical property of materials

Materials	Bending strength	Fracture toughness	Hardness HRA
Al_2O_3	621 ± 97	3.7 ± 0.5	93.0
AF5[a]	633 ± 105	4.1 ± 0.9	93.0
AF10[a]	749 ± 132	5.7 ± 1.2	92.4
AF20[a]	860 ± 117	8.1 ± 1.9	91.5

[a] The figure X in AFX refers to the Fe_3Al content (vol.%) in composite.

The measured results of bending strength σ_f and fracture toughness K_{IC} of monolith Al_2O_3 and Al_2O_3/Fe_3Al composite are shown in Table 1. The σ_f and K_{IC} values of composite containing 20 vol.% Fe_3Al were determined to be 860 MPa and 8.1 MPa $m^{1/2}$, respectively, which were higher than those of pure Al_2O_3 (621 MPa, 3.7 MPa $m^{1/2}$).

The R-curves of the monolith and the composites having 20 vol.% Fe_3Al particles were plotted from the indentation-strength data by using a power law function of K_R versus the crack growth (ΔC), as suggested by Krause [9]. The fracture resistance and the fracture strength σ_f relation are [9]

$$K_r = kc^m \quad (1)$$

$$\sigma_f = AP^{(2m-1)(2m+3)} \quad (2)$$

where k and m are constants, P the indentation load, and A the constant associated with material and crack geometry. It can be seen from Eq. (2) that m can be evaluated from the best-fit slope of the $\log \sigma_f - \log P$ data. The constant k is evaluated from Eq. (1) with the estimated m and the fracture resistance value for a given crack length obtained from the indentation strength

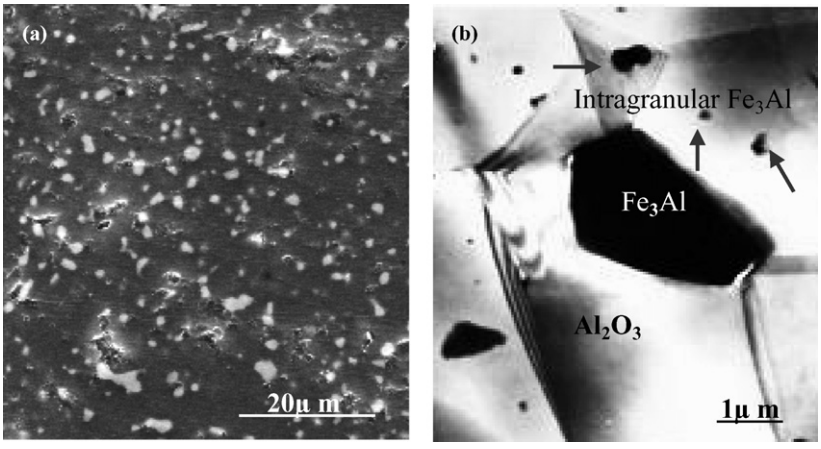

Fig. 1. SEM image (a) and TEM image (b) of Al_2O_3/10 vol.% Fe_3Al composite.

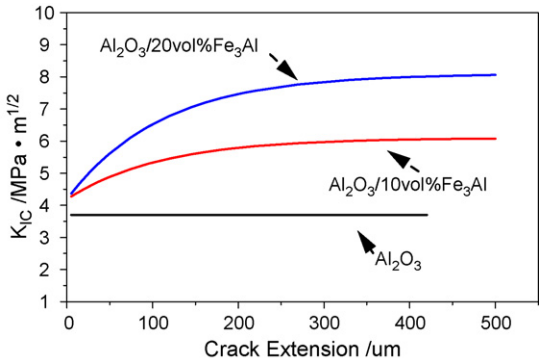

Fig. 2. R-curves of samples.

data. The results are shown in Fig. 2. It can be seen that the R-curve was strongly influenced by the Fe_3Al addition. Significant improvements in the crack growth resistance were achieved by the addition of Fe_3Al particle, thus lead to more pronounced R-curve behavior than pure Al_2O_3.

Indent cracks were made on the polished surface of composite to clarify further the toughening effect that is responsible for the rising R-curve behavior. The crack growth path corresponding with the extended radial cracks of 196 N Vickers indentation on the surface of Al_2O_3/20 vol.% Fe_3Al composite is shown in Fig. 3. Extensive crack interactions, mainly namely crack bridging are observed (Fig. 3(a)), indicating that once the crack has reached the particle–matrix interface, the difference in the crack-tip opening displacement between the ductile particle and the brittle matrix will cause the crack to be locally blunted, thus produce closure stress bridging the crack along its length. These effects require more external load to force the crack propagate further, thus induce the improvement of toughness. In addition, crack deflections that enhance the energy for crack growth were also observed (Fig. 3(b)).

For small-scale bridging, the fracture toughness increment can be estimated from fellow equation: [10]

$$\Delta K_b = \sqrt{E f t \sigma_0 \chi} \tag{3}$$

where E is the elastic modulus of the composites, σ_0 the yield stress, f the volume fraction of bridging particles, t the characteristic dimension of the reinforcement, and χ a dimensionless function representing the work of rupture of the bridging phase. Taking values for E of 370 Gpa for composite with Fe_3Alm, volume fraction f of 0.2, and σ_0 of 450 MPa for Fe_3Al particle [4] the t of 1.3 μm, an estimated value of χ of 0.4 was used. According to Eq. (3) the toughness increment by the grain bridging of Fe_3Al is approximately 4.16 MPa $m^{1/2}$. In addition, the increment in toughness value observed in these composites is also assigned to the thermal residual stress toughening effect resulting from the discrepancy of thermal expansion coefficient between Fe_3Al and Al_2O_3 matrix. The fracture toughness increment arising from the thermal residual stress can be calculated by: [11]

$$\Delta K = 2\sigma_r \sqrt{\frac{2(\lambda - t)}{\pi}} \tag{4}$$

$$\lambda = \frac{1.085t}{\sqrt{f}} \tag{5}$$

where t is the average grain size of toughening phase, λ the average interval of toughening particle, and f the volume fraction of toughening particles. σ_r is the radial pressed stress of matrix, calculated by: [12]

$$\sigma_r = -\frac{\Delta\alpha \Delta T E_m}{(1+\nu_m) + 2\beta(1-2\nu_p)} \left(\frac{R}{r}\right)^3 \tag{6}$$

where $\Delta\alpha = \alpha_p - \alpha_m$, α is the thermal expansion coefficient, the subscript m and P refer to matrix and toughening particle, respectively, υ is the Poisson' ratio, E the Young's modulus, ΔT the difference between the temperature below which the residual stresses cannot be relaxed by diffusional mechanisms (about 600 °C for Fe_3Al) and room temperature, $\beta = E_m/E_P$, R the radius of toughening particles, and r the distance from the centre of a particle of radius R. According to Eqs. (4)–(6), the toughness increment by the residual thermal stress is approximately 0.8 MPa $m^{1/2}$. The sum of the contributions from the crack bridging and the residual thermal stress (4.96 MPa $m^{1/2}$) is close to the toughness difference between the composite having 20 vol.% Al_2O_3 and pure Al_2O_3 (4.4 MPa $m^{1/2}$).

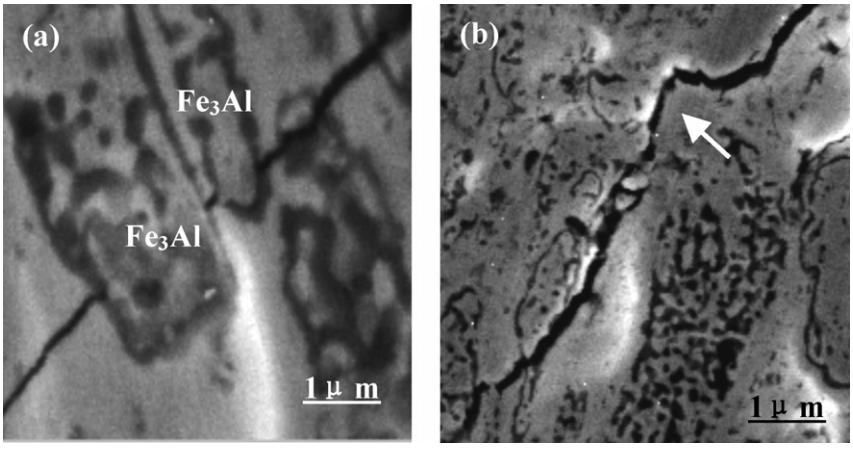

Fig. 3. Indent crack bridging (a) and deflection (b) of Al_2O_3/Fe_3Al composite.

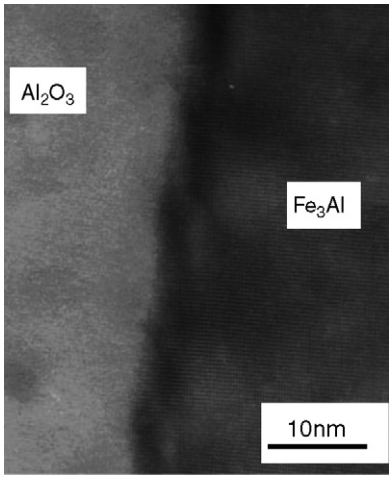

Fig. 4. High-resolution image of the interface between Fe_3Al and Al_2O_3.

Although only a rough estimate, the predicted toughness is comparable to the experimentally measured value.

For bridging toughening mechanism, appropriate ductile particle–ceramic interface bonding is an important factor to achieve optimal toughening effect. High-resolution transmission electron microscopic (HREM) image as shown in Fig. 4 exhibited that no micro-crack was observed at the interface due to the small thermal expansion coefficient mismatch, and no reaction phase (generally induces extremely strong interface bonding sequentially restricting plastically deforming of ductile particle) existed at the interface between Al_2O_3 matrix and Fe_3Al particle. These facts indicate that it is possible to reduce the possibility of premature ductile particle pull-out and, at the same time, ensure appropriate yield deformability of ductile particles during crack propagation, thus obtain optimal toughening effect by Fe_3Al crack bridging.

4. Conclusions

(1) Addition of appropriate content of Fe_3Al intermetallic particles to an alumina matrix induces more pronounced R-curve behavior than pure alumina. The improvement was attributed to the crack bridging and residual thermal stress toughening effect.

(2) No micro-crack was observed at the interface due to the small thermal expansion coefficient mismatch, and no reaction phase (generally induces extremely strong interface bonding sequentially restricting plastically deforming of ductile particle) existed at the interface between Al_2O_3 matrix and Fe_3Al particle.

Acknowledgement

This work is supported by National Natural Science Foundation of China (Grant No. 50572034).

References

[1] R. Cünther, T. Klassen, B. Dickau, Advanced alumina composites reinforced with titanium-based alloys, J. Am. Ceram. Soc. 84 (7) (2001) 509–513.
[2] O. Sbaizero, G. Pezzotti, Influence of residual and bridging stresses on the R-curve behavior of Mo- and FeAl-toughened alumina, J. Eur. Ceram. Soc. 20 (2000) 1145–1152.
[3] R.E. Loehman, K. Ewsuk, A.P. Tomsia, Synthesis of Al_2O_3-Al composites by reactive melt penetration, J. Am. Ceram. Soc. 79 (1996) 27–32.
[4] C.G. McKamey, J.H. DeVan, P.E. Tortorelli, V.K. Sikka, A review of recent developments in Fe_3Al-based alloys, J. Mater. Res. 6 (1991) 1779–1783.
[5] S.H. Ko, R. Ginanamoorthy, S. Hanada, Effect of environment on tensile ductility and fracture toughness of iron aluminides, Mater. Sci. Eng. A222 (1997) 133–139.
[6] A.K. Misra, Identification of thermodynamically stable ceramic reinforcement materials for iron aluminide matrices, Metall. Trans. 21A (1990) 441–446.
[7] Y.S. Yin, J.D. Zhang, J. Li, Mechanical properties of Fe_3Al/Al_2O_3 composite graded coatings, Appl. Surf. Sci. 218 (5) (2003) 345–349.
[8] Y.S. Yin, H.Y. Gong, R.H. Fan, et al., Preparation and mechanical properties of Fe_3Al/Al_2O_3 nano/micro-composite, Trans. Nonferrous Metal Soc. China 13 (6) (2003) 1376–1380.
[9] R.F. Krause, Rising fracture toughness from the bending strength of indented alumina beams, J. Am. Soc. 71 (5) (1988) 338–343.
[10] F.B. Jose, D. Maicos, Influence of the metal particle size on the crack growth resistance in mullite-molybdenum composites, J. Am. Ceram. Soc. 85 (11) (2002) 2778–2784.
[11] M. Taya, S. Hayashi, Toughening of a particulate reinforced ceramic-matrix composite by thermal residual stress, J. Am. Ceram. Soc. 73 (5) (1990) 1382–1391.
[12] J. Selsing, Internal stress in ceramics, J. Am. Ceram. Soc. 44 (8) (1961) 419–421.